

Dr. Jan Wilhelm, Dr. Štěpán Marek, Maximilian Graml

<https://www.ur.de/physics/wilhelm/teaching/sose24-computational-nanoscience>

Computational Nanoscience: Solution to Exercise Sheet No. 8

Exercise 8.1: Geometry

Geometry for 3Å distance:

14

Mg	0.00000000	0.00000000	0.00000000
Mg	-2.14100000	-2.14100000	2.14100000
Mg	-2.14100000	2.14100000	2.14100000
Mg	2.14100000	-2.14100000	2.14100000
Mg	2.14100000	2.14100000	2.14100000
Mg	-4.28200000	-4.28200000	-3.00000000
Mg	-4.28200000	-0.00000000	-3.00000000
Mg	-4.28200000	4.28200000	-3.00000000
Mg	-0.00000000	-4.28200000	-3.00000000
Mg	-0.00000000	-0.00000000	-3.00000000
Mg	-0.00000000	4.28200000	-3.00000000
Mg	4.28200000	-4.28200000	-3.00000000
Mg	4.28200000	-0.00000000	-3.00000000
Mg	4.28200000	4.28200000	-3.00000000

Geometry for 7Å distance:

14

Mg	0.00000000	0.00000000	0.00000000
Mg	-2.14100000	-2.14100000	2.14100000
Mg	-2.14100000	2.14100000	2.14100000
Mg	2.14100000	-2.14100000	2.14100000
Mg	2.14100000	2.14100000	2.14100000
Mg	-4.28200000	-4.28200000	-7.00000000
Mg	-4.28200000	-0.00000000	-7.00000000
Mg	-4.28200000	4.28200000	-7.00000000
Mg	-0.00000000	-4.28200000	-7.00000000
Mg	-0.00000000	-0.00000000	-7.00000000
Mg	-0.00000000	4.28200000	-7.00000000
Mg	4.28200000	-4.28200000	-7.00000000
Mg	4.28200000	-0.00000000	-7.00000000
Mg	4.28200000	4.28200000	-7.00000000

Exercise 8.2: CP2K Input file

```
&GLOBAL
  PROJECT Exc_7
  RUN_TYPE RT_PROPAGATION
&END GLOBAL
&MOTION
  &MD
    ENSEMBLE NVE
    TEMPERATURE 300
    STEPS 1000
    TIMESTEP 0.1
  &END MD
&END MOTION
&FORCE_EVAL
  METHOD QUICKSTEP
  &SUBSYS
    &TOPOLOGY
      &CENTER_COORDINATES
      &END CENTER_COORDINATES
      COORD_FILE_NAME struc.xyz
      COORD_FILE_FORMAT XYZ
    &END TOPOLOGY
    &CELL
      ABC 10 10 20
      PERIODIC NONE
    &END CELL
    &KIND Mg
      BASIS_SET ORB DZVP-MOLOPT-SR-GTH-q2
      POTENTIAL GTH-LDA-q2
    &END KIND
  &END SUBSYS
&DFT
  &EFIELD
    INTENSITY 1000000000000.0
    POLARISATION 0 0 1
    WAVELENGTH 5000.0
    ENVELOP GAUSSIAN
    &GAUSSIAN_ENV
      SIGMA 10.0
      T0 45.0
    &END GAUSSIAN_ENV
  &END
  &REAL_TIME_PROPAGATION
    MAX_ITER 25
    EPS_ITER 1.0E-9
    MAT_EXP TAYLOR
```

```

&END
&PRINT
  &MOMENTS
    PERIODIC .FALSE.
  &END
&END
BASIS_SET_FILE_NAME BASIS_MOLOPT_UCL
POTENTIAL_FILE_NAME GTH_POTENTIALS
&MGRID
  CUTOFF 100
&END MGRID
&SCF
  EPS_SCF 1.0E-7
  MAX_SCF 500
  ADDED_MOS -1
  CHOLSKY INVERSE
  &SMEAR ON
    METHOD FERMI_DIRAC
    ELECTRONIC_TEMPERATURE [K] 300
  &END SMEAR
  &MIXING
    METHOD BROYDEN_MIXING
    ALPHA 0.1
    BETA 1.5
    NBROYDEN 8
  &END
&END SCF
&POISSON
  PERIODIC NONE
  POISSON_SOLVER MT
&END POISSON
&XC
  &XC_FUNCTIONAL LDA
  &END XC_FUNCTIONAL
&END XC
&END DFT
&END FORCE_EVAL

```

Exercise 8.3: Evaluation of the electric field and the dipole moment

- (a) In Fig. 1, we can observe that for 3\AA distance, the time-dependent dipole $p_z^{d=3\text{\AA}}(t)$ follows the field closely, whereas $p_z^{d=7\text{\AA}}(t)$ shows a clear phase-shift of the positive field crest, which we attribute to the tunneling occurring for this geometry.
- (b) The physical reason for the oscillations are interband contributions, i.e. the occupation oscillates indefinitely between occupied and unoccupied bands, since there is no damping mechanism, which dissipates the energy. In Fig. 2, we observe the frequency of the electric field at 60 THz for $p_z^{d=3\text{\AA}}(\omega)$.

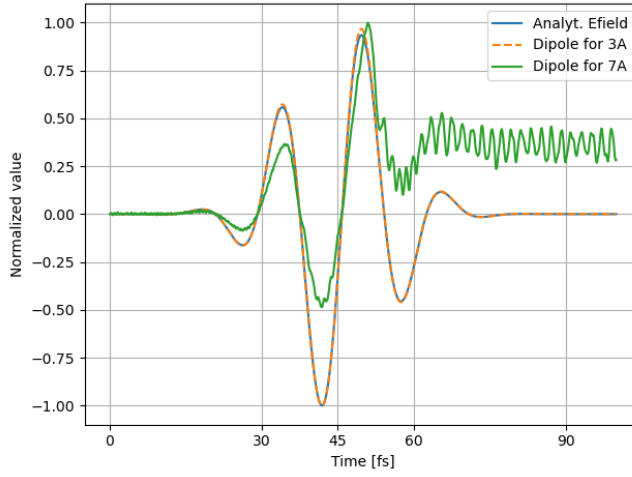


Figure 1: Results of the real-time TDDFT simulation. The dipole for 3\AA distance follows the field closely, whereas the dipole for 7\AA distance shows a clear phase shift as well as oscillations in the right tail.

The frequency-dependent dipole $p_z^{d=7\text{\AA}}(\omega)$ shows additional frequencies, especially a peak at 2.1 eV, which lies in the typical range for the energy differences of the system (cf. next exercise).

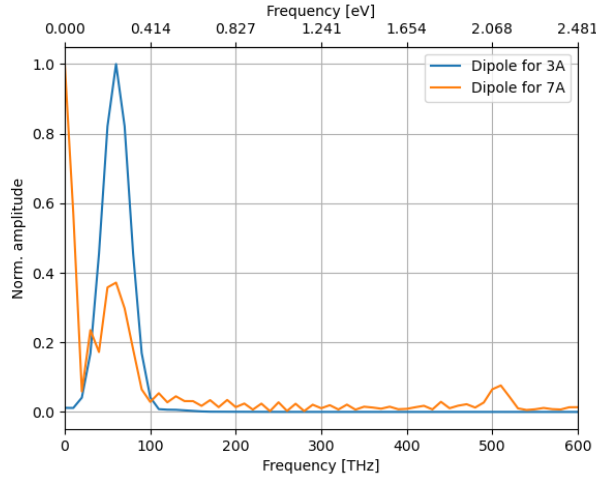


Figure 2: Results of the real-time TDDFT simulation in frequency space normalized to 1. We observe one main peak for $p_z^{d=3\text{\AA}}(\omega)$ at 60 THz, as expected from the time-dependent dipole $p_z^{d=3\text{\AA}}(t)$ in Fig. 1 following the electric field with $\omega_0 = 2\pi \cdot 60$ THz. In contrast, the spectrum of $p_z^{d=7\text{\AA}}(\omega)$ has features in addition to the peak at 60 THz. In particular, the small peak in $p_z^{d=7\text{\AA}}(\omega)$ at 2.1 eV characterizes the oscillations in the right tail of $p_z^{d=7\text{\AA}}(t)$ of Fig. 1.

(c) In order to describe the oscillation of the dipole moment

$$\mathbf{p}(t) = \int d^3r \mathbf{r} n(\mathbf{r}, t), \quad (1)$$

we need to expand the density $n(\mathbf{r}, t) = \sum_i^{\text{occ}} |\psi_i(\mathbf{r}, t)|^2$ in terms of the initial orbitals $\psi_i(\mathbf{r}, t_0) = \varphi_i(\mathbf{r})$, as proposed on the exercise sheet.

We start from the TDKS equation (lecture notes, Eq. (15.16)) after the laser pulse, i.e. $v(\mathbf{r}, t) =$

$\mathbf{d}(\mathbf{r}, t) \cdot \mathbf{E}(t) = 0$:

$$\left[-\frac{1}{2m} \nabla^2 + v_{\text{ext}}(\mathbf{r}) + v_{\text{H}}[n](\mathbf{r}, t) + v_{\text{xc}}[n](\mathbf{r}, t) + v(\mathbf{r}, t) \right] \psi_j(\mathbf{r}, t) = i \frac{\partial}{\partial t} \psi_j(\mathbf{r}, t). \quad (2)$$

By using the stationary KS equation

$$\left[-\frac{1}{2m} \nabla^2 + v_{\text{ext}}(\mathbf{r}) + v_{\text{H}}[n](\mathbf{r}, t) + v_{\text{xc}}[n](\mathbf{r}, t) \right] \varphi_n = \varepsilon_n \varphi_n, \quad (3)$$

$$\hat{h}^{\text{KS}} \varphi_n = \varepsilon_n \varphi_n, \quad (4)$$

we can rewrite Eq. (2) (with $v(\mathbf{r}, t) = \mathbf{d}(\mathbf{r}, t) \cdot \mathbf{E}(t) = 0$ for $t \rightarrow \infty$) as

$$\sum_n \varepsilon_n c_{jn}(t) \varphi_j(\mathbf{r}) = i \frac{\partial}{\partial t} \sum_m c_{jm}(t) \varphi_m(\mathbf{r}), \quad (5)$$

where we expanded

$$\psi_j(\mathbf{r}, t) = \sum_n c_{jn}(t) \varphi_j(\mathbf{r}), \quad (6)$$

since the non-zero electric field in the intermediate time can introduce a mixing of the Ground State KS orbitals.

Using the completeness and orthonormality of the KS orbitals as well as an exponential ansatz, we obtain from Eq. (5):

$$c_{jn}(t) = c_{jn}(t = t_0) e^{-i\varepsilon_n(t-t_0)}, \quad (7)$$

i.e. each coefficient oscillates with a phase given by the respective KS orbital energy.

Reinserting that, we find an interference effect, which leads to the observed oscillations

$$n(\mathbf{r}, t) = \sum_i^{\text{occ}} \left| \sum_{n,m} c_{jn}^*(t-t_0) c_{jm}(t-t_0) e^{i(\varepsilon_n - \varepsilon_m)(t-t_0)} \varphi_n^*(\mathbf{r}) \varphi_m(\mathbf{r}) \right|^2, \quad (8)$$

with the previously discussed characteristic energy scale of the band gap $\varepsilon_n - \varepsilon_m$.

(d) In case, $\mathbf{E}(t) = 0, \forall t$, the stationary KS equation holds at all times and therefore the expansion in Eq. (6) reduces to one coefficient $c_{jn} = \delta_{jn}$. Hence, the density takes the usual form

$$n(\mathbf{r}, t) = \sum_i^{\text{occ}} |\varphi_i^*(\mathbf{r}) \varphi_i(\mathbf{r})|^2, \quad (9)$$

without time dependence, in particular without oscillations.